

Bilateral diffuse uveal melanocytic proliferation associated with endometrial carcinoma – multimodal imaging analysis

Zhi-Peng Cai¹, Hong Zhang¹, Jin-Jing Zhang¹, Chuan-Hong Jie¹, Fang-Tian Dong²

¹Eye Hospital, China Academy of Chinese Medical Sciences, Beijing 100040, China

²Department of Ophthalmology, Peking Union Medical College Hospital, Chinese Academy of Medical Sciences & Peking Union Medical College, Beijing 100730, China

Co-first authors: Zhi-Peng Cai and Hong Zhang

Correspondence to: Hong Zhang. Examination Center, Eye Hospital, China Academy of Chinese Medical Sciences, No. 33 Lugu Road, Shijingshan District, Beijing 100040, China. zhanghong_zhbj@sina.com

Received: 2021-01-08 Accepted: 2022-03-02

DOI:10.18240/ijo.2022.07.25

Citation: Cai ZP, Zhang H, Zhang JJ, Jie CH, Dong FT. Bilateral diffuse uveal melanocytic proliferation associated with endometrial carcinoma – multimodal imaging analysis. *Int J Ophthalmol* 2022;15(7):1209-1213

Dear Editor,

We present a rare case of bilateral diffuse uveal melanocytic proliferation (BDUMP) associated with endometrial carcinoma. BDUMP is a rare paraneoplastic ocular syndrome with generally poor prognosis. Typical features include: 1) multiple subtle, round, or oval red patches in the retinal pigment epithelium (RPE) of the posterior fundus; 2) multifocal areas of early hyperfluorescence corresponding to these patches; 3) development of multiple, slightly elevated pigmented and non-pigmented uveal melanocytic tumours with diffuse thickening of the uveal tracts; 4) exudative retinal detachment; 5) rapid progression of cataracts. These patches progressively increase in size and merge into the giraffe-like pattern characteristic of BDUMP^[1]. Additional signs may be present, including cysts in the ciliary body and iris, dilated episcleral vessels, and a shallow anterior chamber^[2].

The initial presentation of our patient was subtle, but typical signs of BDUMP became apparent in the ensuing 6wk. Multimodal imaging facilitated detection of early signs of BDUMP and provided information on the pathogenesis.

A 79-year-old Chinese woman presented with a 2-month history of bilateral progressive visual deterioration that was worse in the left eye. Her past medical history noted clear cell endometrial carcinoma for which she had undergone hysterectomy 9mo earlier. She had no history of metastasis and not received adjuvant therapy. Her past ocular history included bilateral cataract surgery with insertion of an intraocular lens into the posterior chamber 3mo before presentation.

All procedures adhered to the tenets of Declaration of Helsinki. Written informed consent was obtained from the patients.

On examination, her best-corrected visual acuity was 20/30 in the right eye and 20/60 in the left. Intraocular pressure was 12 mm Hg in both eyes. Slit-lamp examination revealed a shallow periphery in the anterior chamber and pseudophakia in both eyes. Ultrasound biomicroscopy revealed cysts in the ciliary body and iris, diffuse thickening of the ciliary body, and narrowing of the anterior chamber angle (Figure 1A, 1B). Both eyes contained vitreous cells, which were more marked in the left eye. Dilated fundus examination of the right eye was unremarkable but revealed significant vitritis in the left eye without obvious haemorrhage or exudate (Figure 1C, 1D). Near-infrared reflectance (NIR) imaging demonstrated scattered hyperreflective and hyporefective dots in the inferior mid-periphery area bilaterally and around the macula in the left eye (Figure 1E, 1F). Fluorescein angiography (FA) showed a window defect with multiple obstructive speckled pigmented lesions, similarly positioned to the lesions observed by NIR, as well as numerous pinpoint areas of hyperfluorescence in the posterior pole of the right eye (Figure 1G, 1H). Indocyanine green angiography (ICGA) revealed hypofluorescent dots and nevus-like lesions in the early and late phases (Figure 1I, 1J). Spectral-domain optical coherence tomography (OCT) findings were unremarkable in the right eye (Figure 1K) but revealed shallow subretinal fluid in the left macula with similar RPE thickening and loss of the ellipsoid zone (Figure 1L). A provisional diagnosis of Vogt-Koyanagi-Harada disease (VKH) was suspected. The patient was prescribed oral prednisone (60 mg/d for 1wk). However, the therapy failed to improve vision, and the subretinal fluid had increased.

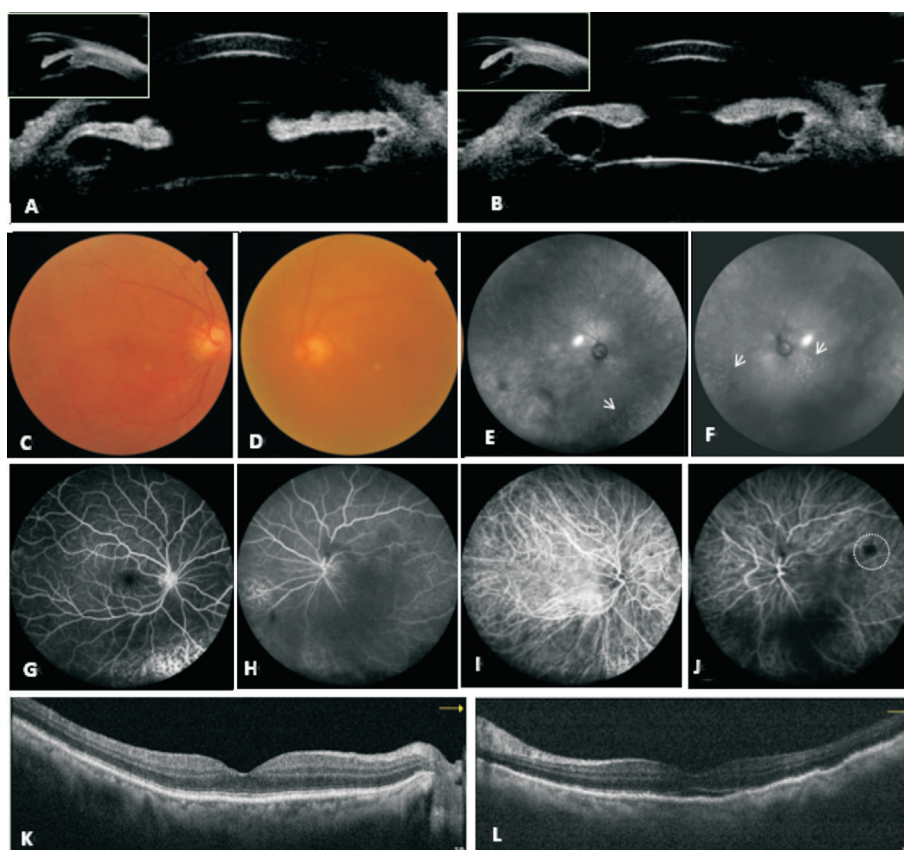


Figure 1 Multimodal imaging upon initial presentation A, B: Ultrasound biomicroscopy images of the right and left eye, respectively, demonstrating cysts in the ciliary body and iris, diffuse thickening of the ciliary body, and narrowing of the anterior chamber angle. C: Fundus photograph of the right eye showing unremarkable findings. D: Fundus photograph of the left eye shows significant vitritis. E, F: NIR images of the right and left eye, respectively, show scattered hyperreflective and hyporefective dots (white arrowheads) in the inferior mid-peripheral area and around the macula in the left eye. G, H: FA images of the right and left eye, respectively, reveal blocking by dotted pigmented lesions within the window defects and pinpoint hyperfluorescence in the posterior pole of the right eye. I, J: ICGA images of the right and left eye, respectively, show blocking by nevus-like lesions (white dashed circle) and dotted pigmentations. K: Spectral-domain OCT image of the right eye shows no obvious abnormalities. L: Spectral-domain OCT image of the left eye reveals shallow subretinal fluid, similar thickening of the RPE, and loss of the ellipsoid zone.

At a follow-up 6wk later, the patient reported bilateral loss of vision. Her visual acuity in both eyes was reduced to hand motion. Fundus examination showed multiple subtle greyish patchy subretinal lesions and a shifting exudative retinal detachment involving the inferior retina and posterior pole in both eyes. The patient underwent a diagnostic vitrectomy combined with silicone oil tamponade for restoration of refractive interstitial transparency and reattachment of the retina.

Three days after surgery, her vision had improved to 20/130 on the right and 20/100 on the left. Fundus examination revealed a giraffe-like pattern with multiple scattered oval or round subretinal greyish patchy lesions separated by polygonal orange pigmentation and nevus-like lesions in both eyes (Figure 2A, 2B). NIR (Figure 2C, 2D) and near-infrared autofluorescence (NIA) images (Figure 2E, 2F) showed numerous polygonal areas of increased intensity consistent with the orange pigmented lesions, within diffuse dark spots corresponding to the greyish patches. Their presence on FA

was the reverse of that observed on NIR and NIA, which showed multifocal patchy window defects surrounded by polygonal hypofluorescence (Figure 2G, 2H). ICGA revealed areas that were blocked by polygonal pigmentations and nevus-like lesions. Furthermore, the nevus-like lesions in the right eye had increased slightly in size (Figure 2I, 2J). OCT angiography showed irregular hyporefective areas in the choriocapillary slab corresponding to the polygonal pigmentations (Figure 2K, 2L). En-face OCT revealed multiple patchy hyporefective lesions bordered by moderately reflective areas in the outer retina slab (Figure 2M, 2N). Spectral-domain OCT with horizontal scans passing through the lesion on en-face OCT demonstrated choroidal thickening. Focal loss of both the RPE and ellipsoid zone corresponded to the hyporefective lesions seen on en-face OCT images, and the thickened adjacent zones corresponded to hyperreflective areas on en-face OCT as well as subfoveal fluid with hyperreflective subretinal deposits in the left eye (Figure 2O, 2P).

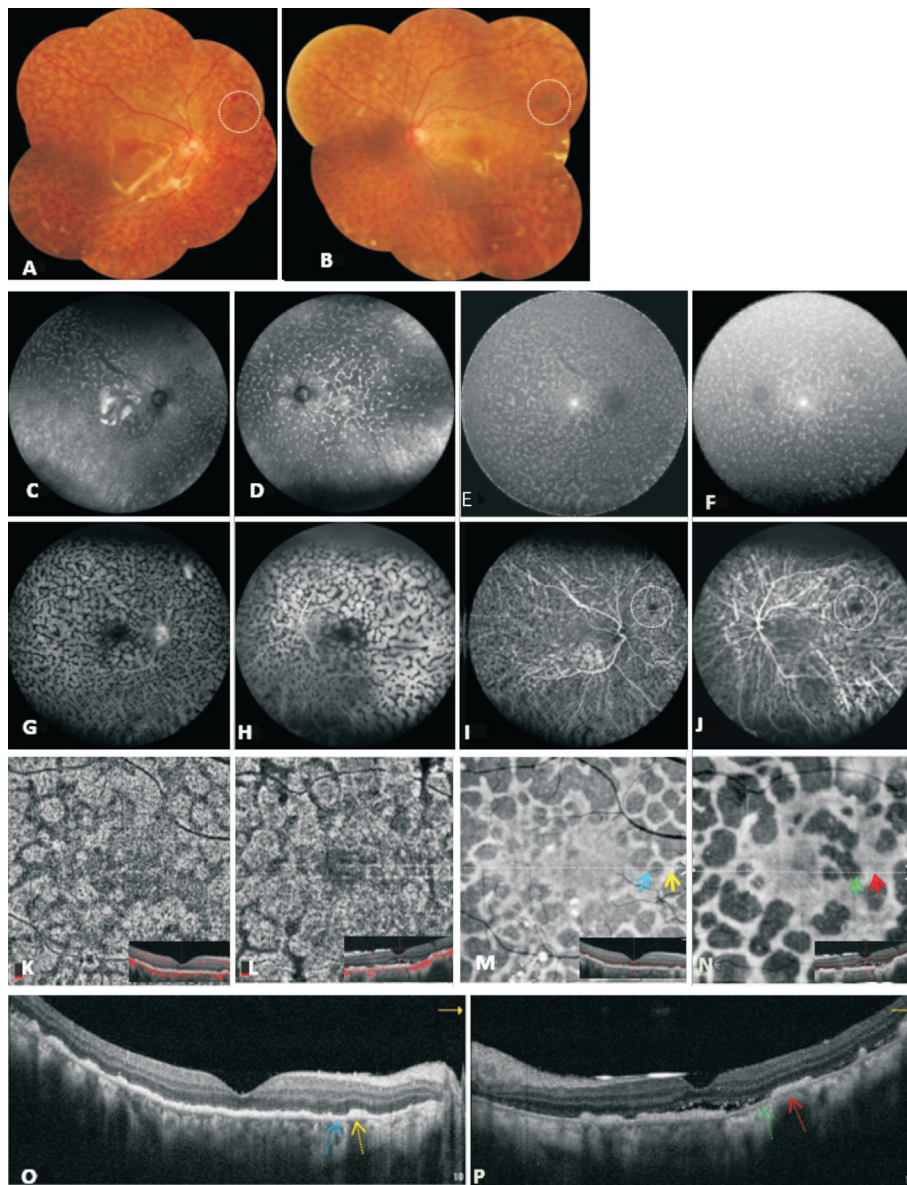


Figure 2 Multimodal imaging 3d after surgery A, B: Fundus montages of the right and left eye, respectively, show a giraffe-like pattern and nevus-like lesions (white dashed circle). C, D: NIR images of the right and left eye, respectively, demonstrate polygonal hyperreflective lesions within diffuse plaque-like dark areas. E, F: NIA images of the right and left eye, respectively, show diffuse plaque-like hypoautofluorescent areas separated by polygonal hyperautofluorescence. G, H: FA images of the right and left eye, respectively, show multifocal patchy window defects surrounded by polygonal hypofluorescence. I, J: ICGA images of the right and left eye, respectively, reveal blocking defects associated with polygonal pigmentations and nevus-like lesions (white dashed circle). K, L: OCT angiography images of the right and left eye, respectively, show polygonal hyporefective areas in the choriocapillary slab. M, N: En-face OCT images of the right and left eye, respectively, show multiple patchy hyporefective lesions (blue and green arrows) surrounded by moderately reflective areas (yellow and red arrows) in the outer retina slab. O, P: Spectral-domain OCT images of the right and left eye, respectively, with horizontal scans passing through the lesion demonstrate choroidal thickening, focal loss of both the RPE and ellipsoid zone (blue and green dashed arrows) corresponding to the hyporefective lesions (blue and green dashed arrows) and thickened adjacent zones (yellow and red dashed arrows) corresponding to moderately reflective areas (yellow and red arrows). Subfoveal fluid is seen with hyperreflective subretinal deposits in the left eye.

Based on these findings, a clinical diagnosis of BDUMP was made. In order to rule out metastatic malignancy and improve vision, extensive investigations for a systemic malignancy and plasmapheresis, which has been the most effective therapy were suggested. However, the patient declined due to financial constraints and did not return for checkup.

BDUMP is a rare paraneoplastic syndrome characterised by a proliferation of benign melanocytes in the uveal tract, which destroys the outer retina and RPE^[1-2]. Its pathogenesis is unclear. Miles *et al*^[3] hypothesised that a specific cultured melanocyte elongation and proliferation (CMEP) factor present in the plasma stimulates growth of melanocytes and that this

factor is probably released by cancer cells or produced by the immune system. A recent report suggests a new aetiology related to high levels of hepatocyte growth factor (HGF) in combination with autoantibodies to α -HGF (anti-69-kDa) may drive choroidal nevi growth and RPE damage^[4].

Notably, the initial presentation in this case was subtle and atypical. It can masquerade as VKH or other retinal pigment epitheliopathy^[1-2], resulting in delayed diagnosis and treatment. Neither systemic steroids nor vitrectomy had any encouraging results in our case. Notably, Cysts in the ciliary body and iris and diffuse thickening of the ciliary body on ultrasound biomicroscopy indicate proliferation of melanocytes in the anterior uveal tract at earlier stages of BDUMP, which may further lead to angle-closure glaucoma and cataracts^[5]. The regions of alternating hyperreflectance and hyporefectance on NIR corresponded to the areas of blocking and window defects seen on FA and the small nevus-like lesions shown on ICGA. These findings are likely caused by degeneration of the RPE and mild choroidal melanocytic infiltration. Spectral-domain OCT showed loss of the ellipsoid zone, thickening of the RPE, and subretinal fluid in the left eye but not in the right macula. This finding suggests that proliferation of melanocytes and obstruction of the RPE and photoreceptors were present before appearance of typical BDUMP signs.

Our case had most of the typical signs of BDUMP except for multiple uveal melanocytic lesions and rapidly demonstrated the presence of the giraffe-like pattern 6wk later. Previous studies^[1,6] had suggested that it probably be a variant of BDUMP where the most outstanding feature was nummular loss of the RPE with minimal to no uveal melanocytic proliferation. Notably, the distinct finding revealed uveal melanocytic proliferation may not be primary cause of the diffuse RPE damage but a direct paraneoplastic process affecting the RPE cells. In our case, the multiple greyish patches corresponded to the window defects seen on FA, loss of both the RPE and ellipsoid zone on spectral-domain OCT, and the dark spots seen on the NIR, NIA, and en-face OCT images, which confirmed destruction of the outer retina and RPE as well as the absence of melanin caused by overlying areas of RPE atrophy. The orange polygonal pigmented lesions corresponded to thickening of the RPE on spectral-domain OCT and the areas of increased intensity seen on NIR, NIA, and en face OCT images, which are caused by aggregation of the adjacent RPE after confluence of the lesions. Furthermore, the slightly enlarged nevus-like lesions seen in the right eye indicated choroidal melanocytic infiltration was progressing slowly. These findings are consistent with previous histopathological findings^[1]. Although Shiraki *et al*^[7] found that the choroidal vasculature in BDUMP was decreased on OCTA, we could not confirm whether the irregular hyporefective area

in the choriocapillary layer represents reduced or halted flow or rather represents an artifact such as from blockage of the flow signal from hyperreflectance of the overlying outer retinal layers and RPE.

Interestingly, the typical giraffe-like pattern took only 6wk to develop in this patient. Potential reasons for this rapid progression are: First, more CMEP factor may have been retained in the subretinal and vitreous due to exudative retinal detachment, leading to proliferation of melanocytes and destruction of the RPE. Second, our patient had not undergone systemic screening for metastatic malignancy, and metastatic cancer cells are suspected to increase secretion of CMEP factor^[3]. Third, it is likely that the diffuse RPE damage is caused by a toxic or immunologic factors are released by the interaction between the carcinoma and the congenital melanocytes^[1]. Finally, autoimmunity generated by cancer cells can combat tumour progression. Therefore, immunosuppression with oral steroids may have an adverse impact on visual symptoms and signs and on long-term survival^[8].

Our case illustrates that multimodal imaging is beneficial for detection of early BDUMP lesions. Ultrasound biomicroscopy may be useful for detecting abnormalities of the anterior uveal tract. NIA and NIR imaging may confirm that the lesions are closely related to the proliferation of melanocytes. En-face and spectral-domain OCT enables better visualisation of the exact location and shape of the structural damage. A combination of NIR, NIA, and en-face OCT imaging is a non-invasive imaging strategy that shows the same typical giraffe-like pattern seen on FA, allowing a more reliable follow-up. This information will contribute to effective treatment and a better understanding of the pathogenesis of BDUMP.

Melanocytic uveal syndrome has been reported associated to many different neoplasms, resulting as a marker of late stages. Reversely, this means that in presence of the syndrome, the patient has to be deeply checked for an eventually misdiagnosed neoplasm. This report adds a new correlation to this well-known association, pinpoint the need to define the common key that in different neoplasms leads to the same ocular syndrome.

ACKNOWLEDGEMENTS

Conflicts of Interest: Cai ZP, None; Zhang H, None; Zhang JJ, None; Jie CH, None; Dong FT, None.

REFERENCES

- 1 Gass JD, Gieser RG, Wilkinson CP, Beahm DE, Pautler SE. Bilateral diffuse uveal melanocytic proliferation in patients with occult carcinoma. *Arch Ophthalmol* 1990;108(4):527-533.
- 2 Klemp K, Kiilgaard JF, Heegaard S, Nørgaard T, Andersen MK, Prause JU. Bilateral diffuse uveal melanocytic proliferation: case report and literature review. *Acta Ophthalmol* 2017;95(5):439-445.

- 3 Miles SL, Niles RM, Pittock S, Vile R, Davies J, Winters JL, Abu-Yaghi NE, Grothey A, Siddiqui M, Kaur J, Hartmann L, Kalli KR, Pease L, Kravitz D, Markovic S, Pulido JS. A factor found in the IgG fraction of serum of patients with paraneoplastic bilateral diffuse uveal melanocytic proliferation causes proliferation of cultured human melanocytes. *Retina* 2012;32(9):1959-1966.
- 4 Niffenegger JH, Soltero A, Niffenegger JS, Yang SF, Adamus G. Prevalence of hepatocyte growth factor and autoantibodies to α -HGF as a new etiology for bilateral diffuse uveal melanocytic proliferation masquerading as neovascular age-related macular degeneration. *J Clin Exp Ophthalmol* 2018;9(4):740.
- 5 Joseph A, Rahimy E, Sarraf D. Bilateral diffuse uveal melanocytic proliferation with multiple iris cysts. *JAMA Ophthalmol* 2014;132(6):756-760.
- 6 Navajas EV, Simpson ER, Krema H, Hammoudi DS, Weisbrod D, Bernardini M, Altomare F. Cancer-associated nummular loss of RPE: expanding the clinical spectrum of bilateral diffuse uveal melanocytic proliferation. *Ophthalmic Surg Lasers Imaging* 2011;42:e103-e106.
- 7 Shiraki A, Winegarner A, Hashida N, Nishi O, Nishi Y, Maruyama K, Nishida K. Diagnostic evaluation of optical coherence tomography angiography and fundus autofluorescence in bilateral diffuse uveal melanocytic proliferation. *Am J Ophthalmol Case Rep* 2018;11:32-34.
- 8 Chan C, O'Day J. Melanoma-associated retinopathy: does autoimmunity prolong survival? *Clin Exp Ophthalmol* 2001;29(4):235-238.